Effect of shape, height, and interparticle spacing of Au nanoparticles on the sensing performance of Au nanoparticle array

Junhua Li (李俊华), Qiang Kan (阚 强)*, Chunxia Wang (王春霞), and Hongda Chen (陈弘达)

State Key Laboratory on Integrated Optoelectronics, Institute of Semiconductors, Chinese Academy of Sciences, Beijing 100083, China

**Corresponding author: kanqiang@semi.ac.cn*

Received February 23, 2011; accepted April 11, 2011; posted online June 16, 2011

The effect of shape, height, and interparticle spacing of Au nanoparticles (NPs) on the sensing performance of Au NP array is systematically investigated. Lengthening the major axis of elliptical NPs with the minor axis kept constant will cause the redshift of the local surface plasmon (LSP) resonance mode, enhance the sensitivity, and widen the resonance peaks. Larger height corresponds to smaller LSP resonance wavelength and narrower resonance peak. With each NP size unchanged, larger interparticle spacing corresponds to larger resonance wavelength and smaller full-width at half-maximum (FWHM). Moreover, duty cycle is important for sensitivity, which is largest when the duty cycle is 0.4.

OCIS codes: 050.5745, 240.6680, 120.7000.

doi: 10.3788/COL201109.090501.

Noble-metal nanoparticle (NP) arrays have been studied extensively in recent years due to their unique optical properties[1]. Local surface plasmon (LSP) resonance refers to the collective oscillations of the conduction band electrons within metallic nanostructures by light[2] and can produce highly enhanced electromagnetic fields in the near-field zone[3,4]. Hence, the positions of LSP resonances are sensitive to the dielectric properties of the medium close to the NPs[5], which have led to the development of NPs as biosensors, applied for analytical purposes in biology, medicine, and chemistry[6−8]. The tunability of their optical properties is of particular importance from a practical viewpoint. The amplitude and spectral position of the LSP resonance of noble-metal NP arrays are greatly affected by the shape, size of metal particles, and the interparticle spacing[1,2]. There are several advantages unique to immobilized regular NP arrays as biosensors: easy control of position and interparticle spacing, and thus the plasmonic properties; no capping agents or stabilizers required and ready for various surface functionalizations; capability for repeated use of the NPs by releasing the absorbed or bounded substances from previous experiments[9]. However, few systematic discussions have been reported on studying the sensing performance of regular NP arrays.

In this letter, we report a systematic investigation on the effect of NP shape, height, and interparticle spacing (defined by P-2R, see Fig. 1(a)) on the sensing performance of Au NP arrays through three-dimensional (3D) finite-difference time-domain (FDTD) simulations using a commercial FDTD software package (FDTD Solutions–Lumerical), in which extinction spectra are calculated by the formula $-10\times\lg(T)$ (T is the normalized transmission) and are used to calculate the resonance wavelength and full-width at half-maximum (FWHM). The wavelength-dependent dielectric constants for Au are obtained from Johnson *et al.*[10]. In each run, the computational window was defined so as to include exactly one repeat unit of the two-dimensional (2D) periodic array centered around a NP. The computational mesh involved a refined region whose mesh sizes in the x–y plane and along the z direction were both set to 2 nm and the mesh accuracy outside the refined mesh region was set to 5. The NP arrays were illuminated at normal incidence with a broadband pulsed excitation having linear polarization along the x direction. Correspondingly, we used antisymmetry boundary conditions in the x direction, symmetry boundary conditions in the y direction, and perfectly matched layers (PMLs) conditions in the z direction to achieve a four-fold reduction in the computational grid size. The array extinction spectra and steady-state field profiles were then calculated from field power monitors and profile monitors at different positions within the computational window. The sensing performance was mainly evaluated from three aspects: resonance wavelength position, sensitivity, and FWHM of the extinction spectra.

Figure 1(a) shows the schematic of the structure simulated and studied in this letter, in which an infinite square array of elliptical Au NPs with pitch P and height H is situated on a K9 glass substrate (refractive index (RI) is 1.5163). In this letter, the major axis of the NPs is parallel to the x axis and its length is denoted by R, while the minor axis is parallel to the y axis and its length r is kept fixed at 70 nm. The superstrate of the structure is homogeneous material, e.g., water. Figure 1(b) is the normalized transmission spectra with superstrate RI (denoted by n) ranging from 1.3 to 1.42 in 0.03 increments, which illustrates the sensing effect of Au NP arrays. The resonance wavelength shifts to the red linearly when n increases, as seen from Fig. 2(b).

In order to study how the shape of NPs influences the sensing performance of the Au NP arrays, we vary the value of R and keep the other parameters constant and then calculate the extinction spectra. As Fig. 2(a) indicates, the resonance wavelength shifts to the red, the corresponding extinction becomes more intense, and the resonance peaks become broader as R increases. Intu-

itively, this can be understood by recognizing that the distance between the excited oscillating charges at the opposite sides of the Au NPs increases with R, thus leading to a smaller restoring force and an increase in the resonance wavelength. The surface coverage of Au NPs will increase with R as well, thus increasing the scattering and intensifying the extinction when LSP resonance occurs. Furthermore, the electric intensity is most intense at the upper and lower corners of the NPs, which correspond to two electric dipoles, one at the metal/air interface and the other at the metal/substrate interface by the field profile. Figure 2(b) is the calculated resonant wavelength plotted versus n (superstrate RI) for the different R indicated in the legend, which shows a fairly good linearity. Figures 2(c) and (d) show that larger R will result in larger sensitivity and FWHM. When R = 70 nm, that is, the particle has a circular shape (R = r), the sensitivity is only 105.2 nm/RI unit (RIU) and the FWHM is also very small at just 8.8 nm. As R increases to 140 nm, sensitivity increases monotonously to 462.8 nm/RIU and FWHM to 59.2 nm. Hence, we can conclude that elliptical NP arrays generally have larger sensitivity and FWHMs than circular NP arrays and that the more elongated the NPs, the larger the sensitivity and FWHM, which is consistent with the experimental results in Refs. [11,12].

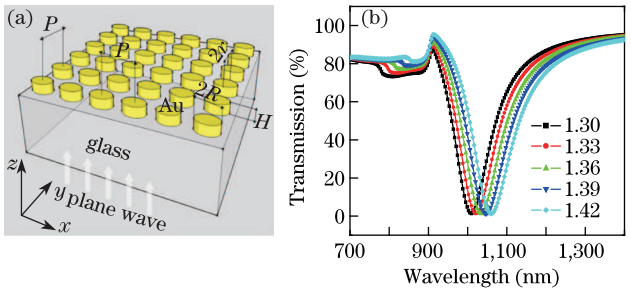

Fig. 1. (a) Schematic of the structures and (b) normalized transmission spectra with superstrate RI ranging from 1.3 to 1.42 in 0.03 increments when R = 120 nm, r = 70 nm, H = 100 nm, and P = 600 nm.

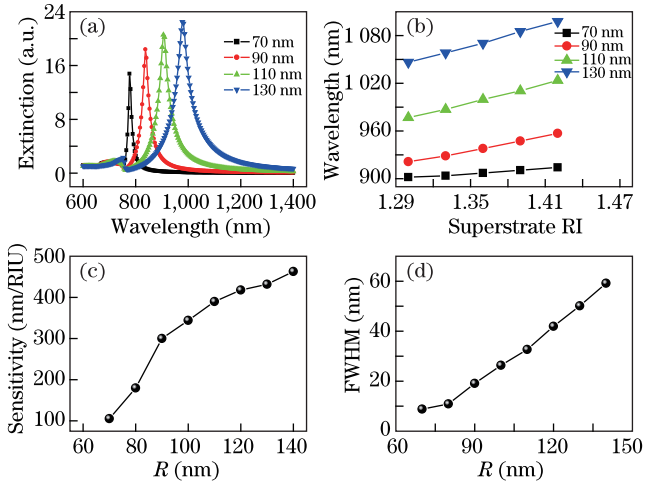

Fig. 2. (a) Extinction spectra for the different R shown in the legend when P = 500 nm; (b) calculated resonance wavelength plotted versus n for the different R shown in the legend when P = 600 nm, (c) sensitivity and (d) FWHM plotted versus R when P = 600 nm. (n = 1.33, r = 70 nm, and H = 100 nm).

To understand these phenomena, we use the quasi-static approximation in solving Maxwell's equation[2] and approximate the NPs as oblate ellipsoids with semi-axes $a_1 = R$, $a_2 = r$, and $a_3 = H/2$, specified by $\frac{x^2}{a_1^2} + \frac{y^2}{a_2^2} + \frac{z^2}{a_3^2} = 1$ in the electrostatic limit. This is rational because the dimensions of the NPs in our study are around 100 nm, while the typical resonance wavelength is around 1 000 nm, much larger than the NPs. A treatment of the scattering problem in ellipsoidal coordinates[2] leads to the following expression for the polarizabilities α along the a_1 principal axis:

$$\alpha = 4\pi a_1 a_2 a_3 \frac{\varepsilon_1 - \varepsilon_\mathrm{m}}{3\varepsilon_\mathrm{m} + 3L_1(\varepsilon_1 - \varepsilon_\mathrm{m})}, \tag{1}$$

where ε_1 and ε_m are the dielectric constants of the ellipsoid material Au and the superstrate, respectively; L_1 is the geometrical factor given by the following:

$$L_1 = \frac{a_1 a_2 a_3}{2} \int_0^\infty \frac{\mathrm{d}q}{(a_1^2 + q)\sqrt{(q + a_1^2)(q + a_2^2)(q + a_3^2)}}, \tag{2}$$

Therefore, the condition for LSP resonance of sub-wavelength ellipsoidal NPs is given by

$$\mathrm{Re}\,[3\varepsilon_\mathrm{m} + 3L_1(\varepsilon_1 - \varepsilon_\mathrm{m})] = 0. \tag{3}$$

The real part of the dielectric function of Au can be expressed as

$$\mathrm{Re}\,(\varepsilon_1) = 1 - \frac{\omega_\mathrm{p}^2 \tau^2}{1 + \omega^2 \tau^2}, \tag{4}$$

where ω_p is the bulk plasmon frequency whose typical value is on the order of 10^{16} rad/s and τ is the relaxation time of the free electron gas, which is typically on the order of 10^{-14} s at room temperature. When the LSP resonant wavelength λ_res is 1 000 nm, $\omega^2\tau^2$ is 355, much larger than 1; thus, we can simplify Eq. (4) to the following formula:

$$\mathrm{Re}\,(\varepsilon_1) = 1 - \frac{\omega_\mathrm{p}^2}{\omega^2}. \tag{5}$$

Combining Eqs. (3) and (5), we can get the expression of λ_res:

$$\lambda_\mathrm{res} = \lambda_\mathrm{p} \sqrt{1 + \left(\frac{1}{L_1} - 1\right) n^2}, \tag{6}$$

where λ_p is the wavelength of the bulk plasmon resonance. Thus, the sensitivity S of ellipsoidal NPs can be calculated as follows:

$$S = \frac{\Delta\lambda}{\Delta n} = \lambda_\mathrm{p} \frac{1}{\sqrt{\left(\frac{L_2}{n}\right)^2 + L_2}}, \tag{7}$$

where $L_2 = L_1/(1 - L_1)$. From Eqs. (6) and (7), the smaller geometrical factor L_1 corresponds to larger resonance wavelength and sensitivity. We have calculated that when R increases from 70 to 150 nm with other parameters kept constant, L_1 decreases from 0.378 to 0.193 monotonously, which can explain why the resonance wavelength and sensitivity of elliptical NP arrays increased with R. Increasing R will shorten the spacing of neighboring NPs, but the effect of shape on the

transmission spectra is much larger than the interparticle spacing by our calculation that we can ignore the effect of small change in spacing caused by increasing R. In addition, FWHM is governed by the lifetime of the resonance mode as $\Gamma = \hbar/\tau$, where τ is the lifetime and Γ (in unit of eV) represents the FWHM. The broadening of the peaks with the increase in R can be ascribed to the fact that larger R will give rise to larger scattering and thus larger radiative decay, which will result in a shorter lifetime τ and thus larger FWHM.

From the discussions above, we know that the shape of the NPs influences the sensing performance significantly. In terms of the effect of height, Fig. 3(a) shows the extinction spectra of different heights with other parameters constant and indicates that as the height increases, the main resonance wavelength (corresponding to the maximum extinction) experiences a blueshift. A simple interpretation can also be constructed based on the harmonic oscillator model of localized plasmonic excitations. As the height increases, the amount of charges induced on both sides by the incident optical field increases while their separation remains fixed. As a result, the displaced electron gas experiences a larger restoring force, leading to a shorter resonance wavelength[13]. Using Eqs. (2) and (6), such a blueshift can be predicted. As height increases from 60 to 260 nm, the geometrical factor L_1 increases monotonously from 0.188 to 0.318, thus the resonance wavelength decreases with height according to Eq. (6). Figure 3(a) also indicates that the extinction is more remarkable for taller NPs. Moreover, a second weaker extinction peak appears and redshifts as height increases, which can be interpreted in terms of the interaction of electric quadrupoles[13]. Figure 3(b) shows that sensitivity increases with height at first, but when the height reaches 140 nm, the sensitivity begins to decrease with height. At the same time, FWHM decreases with height monotonously, as can be seen from Fig. 3(c). This may be due to the fact that larger height corresponds to smaller resonance wavelength, and thus a smaller imaginary part of the dielectric constant of Au in the wavelength region concerned, resulting in a weaker absorption that tends to lengthen the lifetime of the resonance mode. However, the extent of this variation is very small compared with the case of changing R, which suggests that the extinction when resonance occurs involves an interaction of light primarily with the top or the bottom surface. Therefore, height exerts a relatively weaker influence on sensitivity and FWHM.

To discuss the effect of interparticle spacing, we vary the pitch (P) of NP arrays, but the size of each single NP is kept constant. Figure 4(a) shows the extinction spectra when P varies from 500 to 800 nm, and several features are apparent. First, the Au NP arrays exhibit a pronounced redshift as P increases, and the redshift is more remarkable for larger pitches, namely larger interparticle spacing. The field of each NP is the sum of the incident field and the retarded dipole and multipole fields of all the other particles with their respective phase shifts through which the coupling between the NPs is obtained. The general effect of the far-field dipolar coupling tends to blueshift the resonance wavelength[14]. When P increases, the fields contributed by other NPs are smaller and thus the coupling is weaker; the resonance position

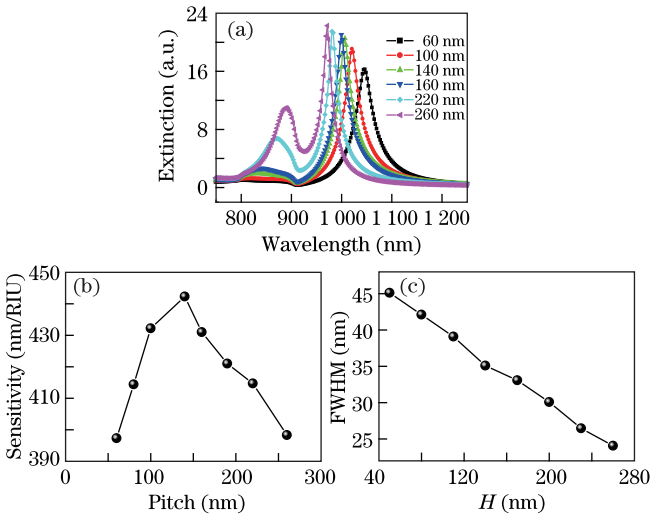

Fig. 3. (a) Extinction spectra for the different heights shown in the legend; (b) sensitivity and (c) FWHM plotted as a function of height. (P = 600 nm, R = 120 nm, r = 70 nm, and n = 1.33).

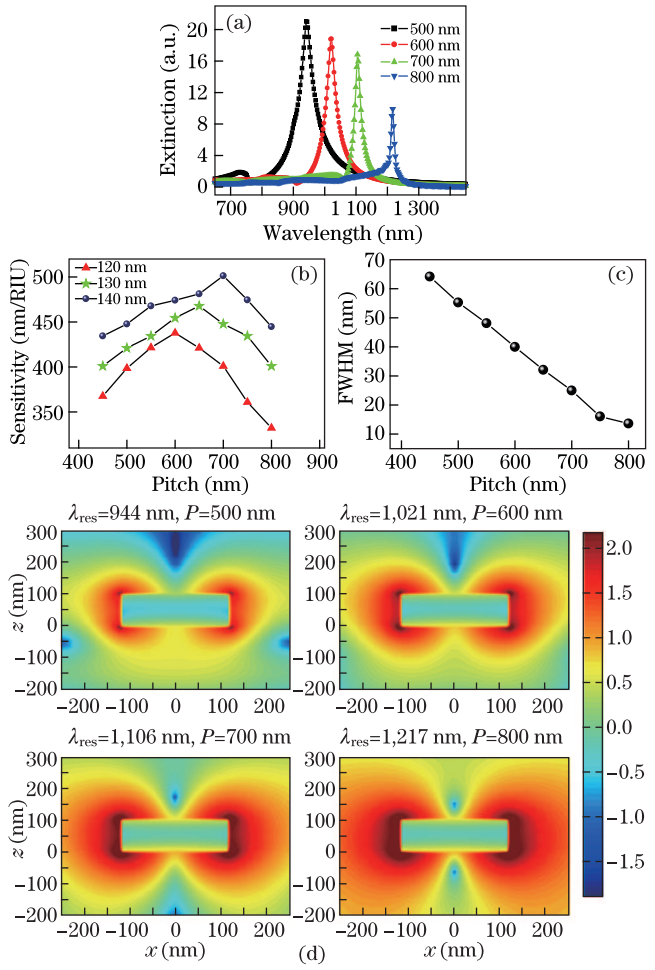

Fig. 4. (a) Extinction spectra for the different pitches shown in the legend when R = 120 nm; (b) sensitivity plotted versus the pitch for R = 120, 130, and 140 nm, respectively; (c) FWHM plotted versus the pitch when R = 120 nm; (d) (color online) lg-scale plots of electric field intensity on the x–z plane through the center of the NPs with the same color bar for four different pitches with R = 120 nm when the resonance occurs. (n = 1.33, H = 100 nm, and r = 70 nm).

then shifts to the red. Second, the extinction is weaker and the resonance peaks are narrower for larger interparticle spacing. Figure 4(b) shows the trend that sensitivity varies with P, in which sensitivity reaches a maximum when $P = 600$, 650, and 700 nm for $R = 120$, 130, and 140 nm, respectively. Interestingly, in all the above cases, duty cycles are 0.4, which suggests that duty cycle is important in determining sensitivity. In Fig. 4(c), FWHM decreases monotonously as P increases, which can be understood considering that weaker coupling between NPs of larger pitches will lengthen the lifetime of the resonance mode. Figure 4(d) is the lg-scale plots of electric field intensity distribution on the x–z plane through the center of the NPs using the same color bar for four different pitches with $R = 120$ nm, $H = 100$ nm, and $n = 1.33$. It is clear that when resonance occurs, the electric field intensity is stronger for larger pitches, which indicates that larger interparticle spacing corresponds to larger field enhancement with each NP size unchanged. This is in agreement with the experiment results of Ref. [15] and can be explained as follows. Quality factor (Q) is defined by $\lambda_{\rm res}$/FWHM. When the pitch increases, $\lambda_{\rm res}$ increases, while FWHM decreases; therefore, Q is larger for larger interparticle spacing. Q also represents the enhancement of the incident light field, thus larger interparticle spacing corresponds to larger field enhancement.

In conclusion, shape, height, and interparticle spacing are three important factors that work together in determining the sensing performance of NP arrays. Elliptical NP arrays have larger sensitivity than circular ones. When the minor axis length is kept constant, the larger the length of the major axis is, the larger will be the sensitivity, FWHM, and resonance wavelength. Increasing the height of NPs will blueshift the resonance wavelength and narrow the resonance peaks. However, the influence of height on sensitivity and FWHM is much weaker compared with shape. With each NP size unchanged, larger interparticle spacing corresponds to larger, stronger field enhancement and smaller FWHM. Moreover, duty cycle is important for sensitivity, which is largest when duty cycle is 0.4. These results are relatively instructive and meaningful when using NP arrays in sensing applications.

This work was supported by the National Natural Science Foundation of China (Nos. 60736037, 60978067, 60807010, and 61036009), the National "973" Project of China (Nos. 2009CB320300 and 2010CB934104), and the National "863" Program of China (No. 2009AA03Z412).

References

1. U. Kreibig and M. Vollmer, *Optical Properties of Metal Clusters* (Springer, Berlin, 1995).
2. C. F. Bohren and D. R. Huffman, *Absorption and Scattering of Light by Small Particles* (John Wiley and Sons, New York, 1983).
3. H. Zhao and D. Yuan, Chin. Opt. Lett. **8,** 1117 (2010).
4. Z. Zhou, Q. Tan, and G. Jin, Chin. Opt. Lett. **8,** 1178 (2010).
5. N. G. Khlebtsov, L. A. Trachuk, and A. G. Mel'nikov, Opt. Spectros. **98,** 77 (2005).
6. A. J. Haes, W. P. Hall, L. Chang, W. L. Klein, and R. P. Van Duyne, Nano Lett. **4,** 1029 (2004).
7. Y. Zhou, H. Xu, A. B. Dahlin, J. Vallkil, C. A. K. Borrebaeck, C. Wingren, B. Liedberg, and F. Höök, Biointerphases **2,** 6 (2007).
8. J. Yan, Y. Lu, P. Wang, C. Gu, R. Zheng, Y. Chen, H. Ming, and Q. Zhan, Chin. Opt. Lett. **7,** 909 (2009).
9. E. Hutter and J. H. Fendler, Adv. Mater. **16,** 1685 (2004).
10. P. B. Johnson and R. W. Christy, Phys. Review B **6,** 4370 (1972).
11. Y. B. Zheng, B. K. Juluri, X. Mao, T. R. Walker, and T. J. Huang, J. Appl. Phys. **103,** 014308 (2008).
12. P. Hanarp, M. Käll, and D. S. Sutherland, J. Phys. Chem. B **107,** 5768 (2003).
13. J. Henson, J. DiMaria, and R. Paiella, J. Appl. Phys. **106,** 093111 (2009).
14. B. Lamprecht, G. Schider, R. T. Lechner, H. Ditlbacher, J. R. Krenn, A. Leitner, and F. R. Aussenegg, Phys. Rev. Lett. **84,** 4721 (2000).
15. C. Hägglund, M. Zäch, G. Petersson, and B. Kasemo, Appl. Phys. Lett. **92,** 053110 (2008).